

Characterization of SPCC Steel Stress Behaviour in Brine Water Environment

Chien-Hung Lin^{1,*}, Jia-Ren Lee²

¹ Department of Physics, ROC Military Academy, Feng-Shan, Kaohsiung, Taiwan

² Department of Physics, National Kaohsiung Normal University, Kaohsiung, Taiwan

*E-mail: linhungcma@gmail.com

Received: 7 July 2018 / Accepted: 22 August 2018 / Published: 7 February 2019

Stress corrosion cracking of steel-plate cold-rolled commercial (SPCC) steel during slow-strain-rate tests (SSRT) in two conditions, i.e., in air and brine water, was investigated in this study. SSRT was employed to discuss the plastic sensitivity of SPCC steel in brine water (0.5, 3, 6, 9 and 18 wt%). The effect of brine water on the microstructure, fracture surface, and corrosion resistance of SPCC steel were observed by microscope and potentiodynamic polarization measurement. The necking phenomenon and dimples were observed by optical microscopy and scanning electron microscopy, and the fracture surface existed in ambient air. Hence, the results revealed that SPCC steel possesses superior strain energy and ductile behaviour in ambient environment. In comparison, the specimens underwent rigorous deterioration of mechanical properties during SSRT in brine water. Furthermore, the irregular profile and cleavage regions on the fracture surface were caused by the uniaxial force and synchronous corrosion of the specimen in brine water. The effect of concentration on the corrosion resistance was evaluated by open-circuit and potentiodynamic measurement in the presence of brine water. The inferior mechanical properties of SPCC steel were caused by the weaker corrosion resistance in the NaCl solution (3 wt%). A comparison between the analytical and experimental results showed agreement. This achievement promotes the development of SPCC steel in the near future.

Keywords: Stress corrosion cracking (SCC), SPCC steel (steel-plate cold-rolled commercial), slow-strain-rate test (SSRT), fracture surface, brittle

1. INTRODUCTION

In recent years, steel-plate cold-rolled commercial (SPCC) steel has been extensively applied to vehicle structures owing to its mechanical properties. However, cold-working treatment decreases the corrosion resistance of SPCC steel owing to artificial defects on the surface. The corrosion resistance of steel has been discussed by abundant literature [1-3]. Localized corrosion occurs on the deformation

plane because the carbon atom migrates to the faulty position. The mechanical property of SPCC steel is subject to refinement of grain size due to the addition of rare elements. The stability of a rust layer is caused by the presence of α -FeOOH phase, and the corrosion resistance of SPCC steel is modified by the addition of lanthanum and cerium elements [4]. Induction heat treatment has been employed to modify the quality of SPCC steel surface [5]. The grain size of SPCC steel was evaluated by atomic force microscopy (AFM), which showed the grain refinement mechanism after the induction heat treatment. In essence, the mechanical property is inversely proportional to the grain size according to the Hall–Petch relationship. A superior mechanical property is necessary for the structure of dynamic machines and vehicles, and corrosion resistance is a crucial factor for development in the oceanic environment. There is synergism between a corrosive environment and static stress on SPCC steel subjected to the SCC over time. SCC also results in fatal accidents and decreased human safety. For the prevention of SCC, a policy is required to ensure reasonable service life in product design. SCC in brine environment has been discussed in the literature [6-12].

SSRT has been employed to evaluate the stress corrosion of AISI 316L austenitic stainless steel, in which the specimen was immersed in a boiling $MgCl_2$ environment [13]. The specimen was susceptible to embrittlement, and the transgranular and intergranular fracture modes could be observed on the failure surface. Electrochemical noise measurement and SSRT were executed to discuss the SCC susceptibility of X-52 carbon steel in an environment based on E95 blend (5 V% gasoline and 95 V% ethanol) mixed with water (0.5, 1, 2, 5, 10, and 20 V%). When the water content was lower than 2 V%, secondary cracking could be observed on the specimen. The uniform corrosion process is correlated with anodic and cathodic fluctuations electrochemical noise with increasing water content in E95 blend [14]. The open-circuit potential (OCP) and corrosion potential tests have been employed to discuss SCC, in which the stress was loaded onto the specimen simultaneously [15]. X80 pipeline steel was plunged into the soil-simulating environment, and alkaline soil was obtained from Daqing City (in China). From the OCP, the potentials of the X80 pipeline steel with and without 550 MPa external stress were -0.7 and -0.8 V, respectively. In addition, the corrosion current and potential dramatically varied with the stress according to potentiodynamic measurement.

The effect of temperature on UNS S41425 supermartensitic stainless steel was evaluated in 3.5 wt% NaCl solution with sodium sulphide (Na_2S), and electrochemical impedance spectroscopy (EIS) was employed to study sulphide stress corrosion cracking (SSCC) behaviour [16]. The steel was austenitised at 932 °C for 60 min and then tempered at 611 °C for 11 h before air cooling. According to the SEM image, the steel was susceptible to brittleness on the fracture surface and intergranular cracking at 80 °C. According to the EIS, the electron transfer resistance increased with increasing elastic behaviour and then decreased with increasing stress before failure. The SCC behaviour of 40CrNi₂Si₂MoVA and 30CrMnSiNi₂A steel was compared by SSRT [17], and the corrosion environment was dominated by neutral 3.5 wt% NaCl solution. Meanwhile, the gauge section was polished by emery paper to 800 grits, and the polarization potential was loaded as OCP, -550 , -700 , -850 , and -1000 mV with respect to a KCl saturated calomel electrode (SCE). Both 40CrNi₂Si₂MoVA and 30CrMnSiNi₂A steel were susceptible to hydrogen-induced cracking during the OCP measurement. The specimen demonstrated a ductile character when the polarization potential to load was -550 mV, yet others were susceptible to brittle fracture with SSRT. The SCC of DSS AISI 318 duplex stainless

steels (DSS) was investigated by SSRT with a 10^{-6} /s strain rate in a 115000 ppm chloride solution [18]. The corrosion currents of the DSS at 25 and 70 °C were 2.7×10^{-7} and 8.0×10^{-6} A /cm², respectively. The ultimate strength of the DSS decreased with increasing cathodic potential. A dynamic tensile test (strain ranging from 10^{-2} to 10^{-6} s⁻¹) was employed to investigate the crack initiation of mild steel [19]. The degradation of the mechanical property was strongly related to the high strain rate owing to the formation of abundant dislocations. With the hydrogen-induced cracking mechanism, higher strain was demonstrated in the corrosive environment than in air during SSRT. The hydrogen embrittlement susceptibility of UNS N07718 (Alloy 718) was investigated in substitute ocean water [20]. The specimen was precharged with hydrogen for 4 or 16 weeks at cathodic potential of -1.1 V relative to an SCE. Furthermore, the strain energy of the specimen with precharge obviously decreased as the hydrogen was infused into the surface of the specimen.

Hence, the goal of this research is to discuss the SCC behaviour of SPCC steel under brine water. When SSRT is below the critical strain rate, brittle failure can be observed on the SPCC steel. This achievement warrants the fundamental design of SPCC steel as a part of manufactured development in the near future.

2. EXPERIMENTS

The test material of this study was SPCC steel with cold-rolling treatment, and the chemical composition (wt%) of the tested material is listed in Table 1.

Table 1. Chemical composition (mass fraction) of SPCC steel

Element	C	Si	Mn	S	P
Weight %	0.12	0.5	0.5	0.025	0.035

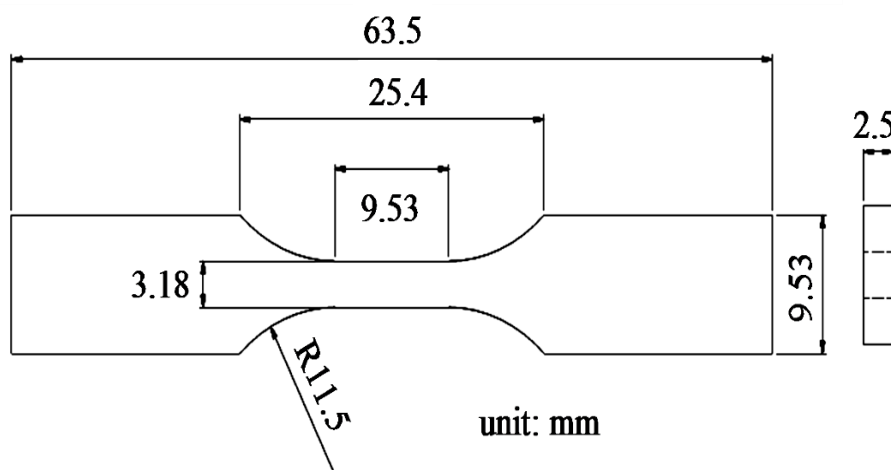


Figure 1. Geometry and dimensions of the tensile specimen

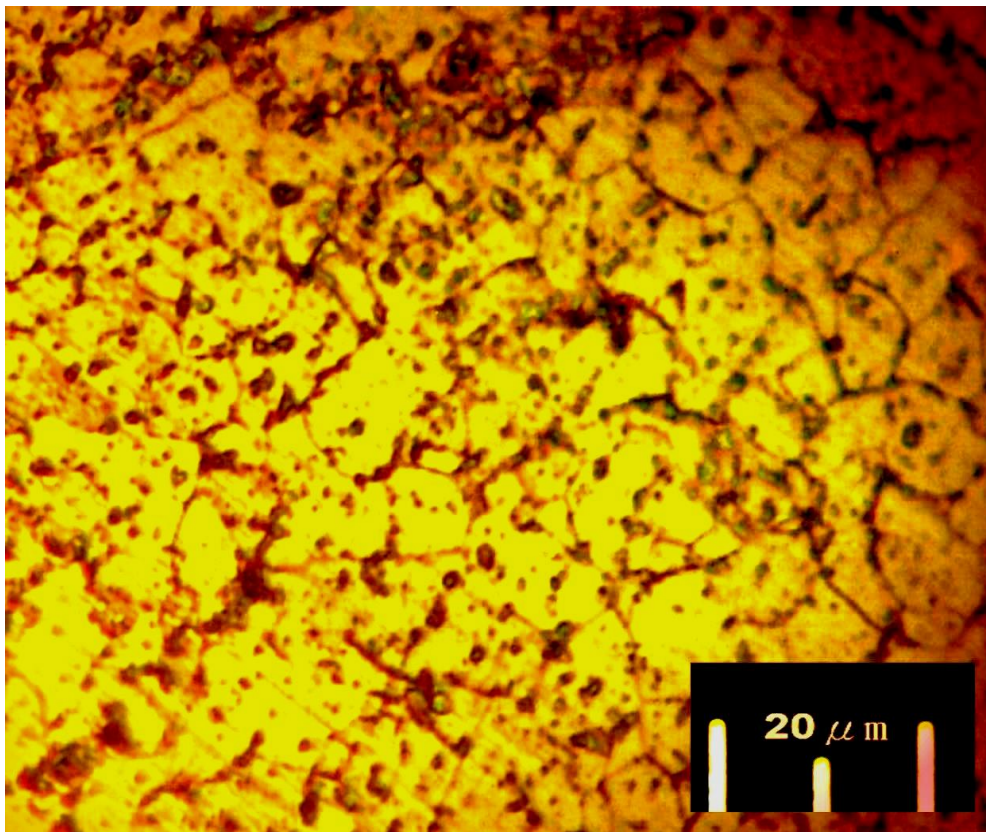


Figure 2. Optical images of the SPCC steel microstructure

The geometry of the specimen was machined as shown in Fig.1, and the gauge section was 2.5 mm in thickness. In this work, the steel was heat-treated with an annealing process at 500 °C for 2 h before air cooling to diminish the inner stress. The surface of the specimen was ground by emery paper to 800# grit and rinsed with deionized water to reduce the artificial defects on the specimen surface. Finally, the specimen was degreased with acetone and dehydrated under a stream of hot air (65 °C) for 1 h. The metallographic structure and the coexistence of ferrite and carbides at the surface of the specimen are demonstrated in Fig. 2.

2.1 Electrochemical test

Electrochemical measurements were carried out in NaCl solutions (weight concentration 0.5, 1.5, 3, 6, 9, and 18 wt%) using a Versastat 4 system (AMETEK Inc). The corrosion resistance of the SPCC steel was measured by potentiodynamic polarization at ambient air temperature. The SPCC steel was machined into a 1 cm² sample and rinsed with deionized water before the electrochemical test. A standard three-electrode system containing the SPCC steel as the working electrode, a platinum electrode (auxiliary electrode), and an Ag/AgCl electrode (reference electrode) was used. In the potentiodynamic polarization test, the sweeping potential and scan rate were -1.1 to 0.2 V and 0.5 mV/s, respectively. The OCP was performed for 5000 s to investigate the stability of the oxide film on the specimen.

2.2 Mechanical test

The stress corrosion cracking susceptibility was investigated by SSRT (strain rate $5.5 \times 10^{-7} \text{ s}^{-1}$) in the NaCl solution (weight concentration 0.5, 1.5, 3, 6, 9, and 18 wt%) at room temperature as shown in Fig. 3. Mechanical properties including the yield point and ultimate tensile strength were characterized by the stress–strain curve.

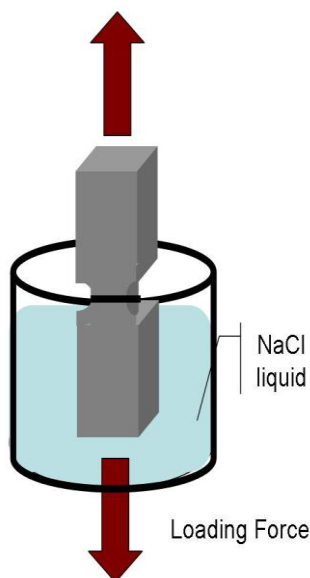


Figure 3. A schematic diagram of the experimental apparatus for SSRT

3. RESULT AND DISCUSSION

3.1 Corrosion resistance

The effect of NaCl concentration on the corrosion process of SPCC steel was investigated using potentiodynamic polarization. These data (anodic and cathodic Tafel slopes \hat{a}_a and \hat{a}_c , corrosion potential E_{corr} , and corrosion current density i_{corr}) characterize the relevant properties responsible for the corrosion resistance of SPCC steel as listed in Table 2.

Table 2. Corrosion characteristics of SPCC steel under different concentrations (wt%) of NaCl by potentiodynamic polarization measurements

NaCl(wt%)	E_{corr} (V) vs SCE	I_{corr} (A/cm ²)	\hat{a}_a (V/dec)	\hat{a}_c (V/dec)
0.5	-0.76	2.61E-5	0.117	-0.262
3	-0.72	3.75E-5	0.115	-0.223
6	-0.60	1.34E-6	0.156	-0.118
9	-0.49	9.34E-8	0.202	-0.082
18	-0.47	7.44E-8	0.152	-0.225

The E_{corr} values for the SPCC steel specimens in 3 and 18 wt% NaCl concentration were -0.72 and -0.47 V, respectively. It appears that E_{corr} decreased in the lower NaCl concentration owing to its active surface in brine water. The corrosion current densities for the SPCC steel specimens in 3 and 18 wt% NaCl concentration were $3.75\text{E}-5$ and $7.44\text{E}-8$ (A/cm^2), respectively. The corrosion potential and corrosion current shifted as depicted in Fig. 4.

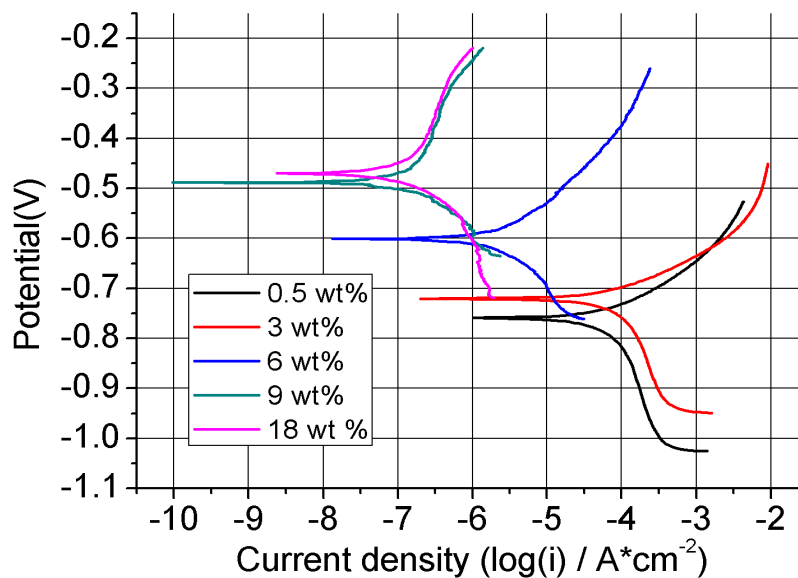


Figure 4. Potentiodynamic corrosion testing of SPCC steel in brine water (sweeping potential from -1.1 to 0.2 V)

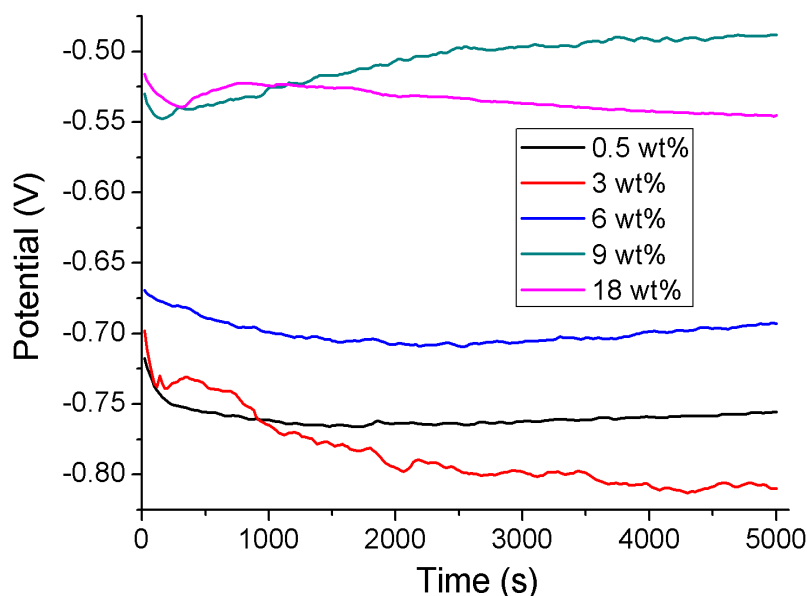


Figure 5. Time dependence on open-circuit potential of SPCC steel in NaCl solution for 5000 seconds.

The corrosion current of the SPCC steel subjected to the 18 wt% NaCl was as much as three orders of magnitude less than that of the 3 wt% NaCl. Even the solution conductivity increased with

increasing NaCl concentration, yet the relative corrosion rate depended on the NaCl concentration and the dissolved oxygen. When the NaCl content exceeded 3 wt% in the solution, the solubility of dissolved oxygen decreased with increasing dissolved salt content [21]. Furthermore, the OCP shifts to the positive direction with increasing NaCl content. Hence, a saddle point existed in the relative corrosion rate versus the NaCl content. The open-circuit test was employed to investigate the growth kinetics of oxide film on the specimen. Fig. 5 presents the chronological change of the open circuit as a function of time for NaCl contents of 0.5, 3, 6, 9, and 18 wt%. It is clear in Fig. 5 that a steady state is approached asymptotically, yet the curve (approximately 3 wt% after 4000 s) still has an unstable status [2]. This result is because the curve is strongly related to the passive film on the specimen, so the thickness of the film varied with time during the electrochemical reaction [6]. The present result indicates that NaCl content of 3 wt% is a severe environment for steel [3].

3.2 Mechanical properties

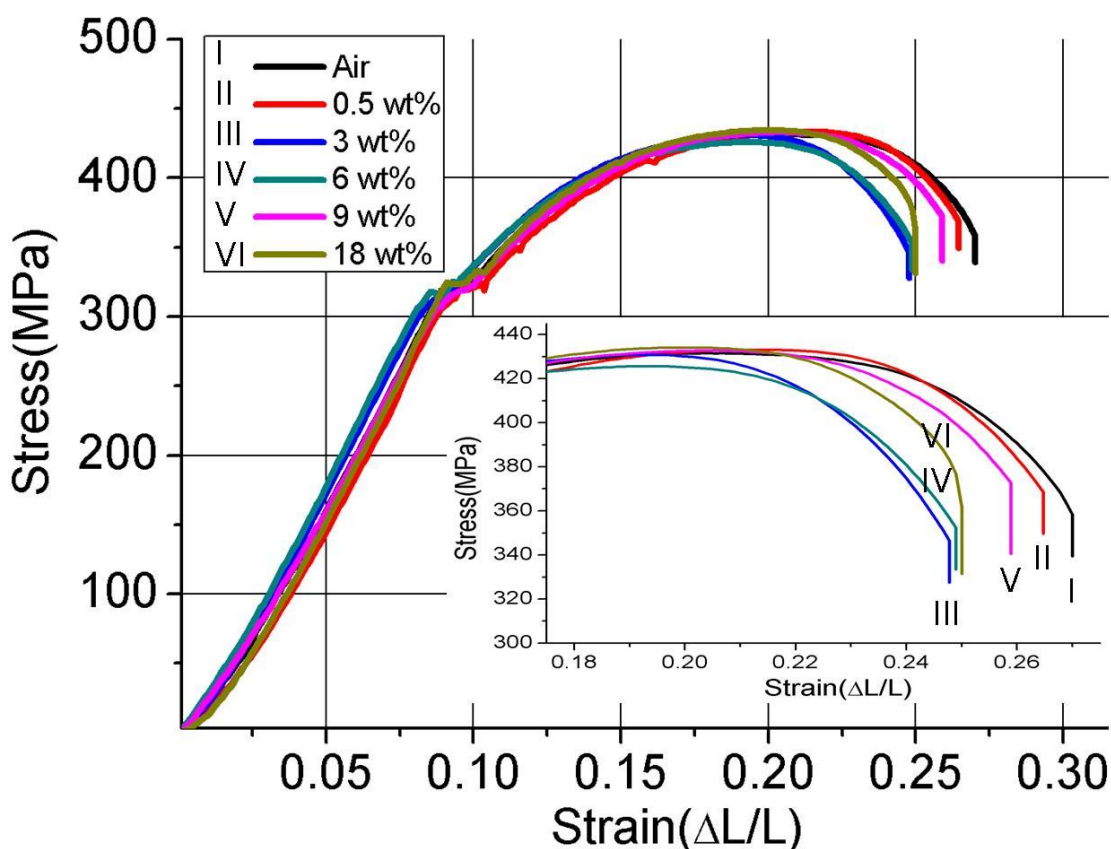


Figure 6. Slow strain rate test (strain rate $5.5 \times 10^{-7} \text{ sec}^{-1}$) results for SPCC steel exposed to brine water with various NaCl concentrations (wt%)

The SSRT was executed in brine water environment at a fixed strain rate (strain rate $5.5 \times 10^{-7} \text{ sec}^{-1}$) until its fracture. The dependence of stress and strain on different values of NaCl concentration is shown in Fig. 6. With changes in the yield platform, the irreversible transition between the elastic and plastic regions renders the movement of dislocations [19]. There was a minor difference in the yield

platform between curves owing to the initial stage of the corrosion process. Eventually, the increasing stress continued to act on the specimen until the failure point. It is obvious in Fig. 6 that the mechanical property of steel deteriorated in the brine water [17].

Table 3. Tensile properties obtained for SPCC steel exposed to brine water with various NaCl concentrations (wt%) at room temperature

NaCl concentration (wt%)	Yield Strength (MPa)	Ultimate tensile strength (MPa)	Strain (%)	Failure time (hour)
Atmospheric environment	318.5	431.2	27.1	76.1
0.5	308.7	433.2	26.4	65.6
3	294.0	430.2	24.7	63.9
6	316.5	425.3	24.9	64.2
9	306.7	432.2	25.9	65.0
18	323.4	434.1	25.0	62.7

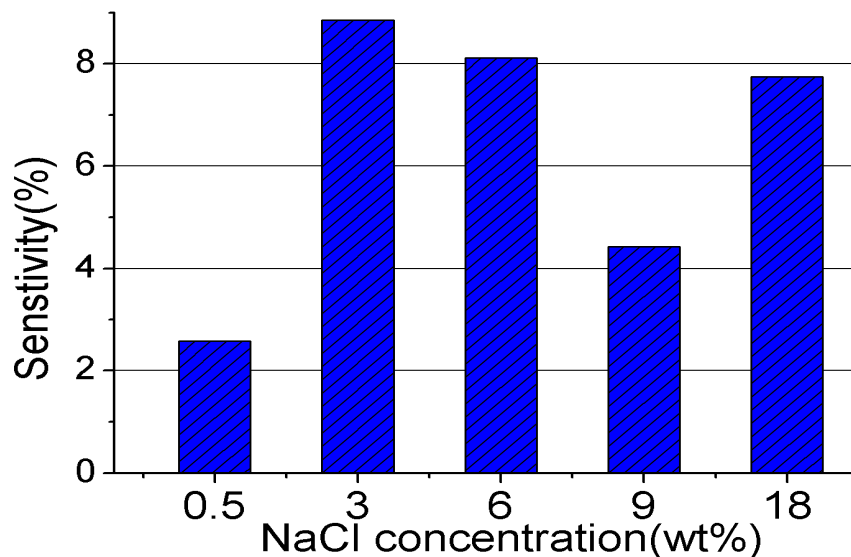


Figure 7. Sensitivity index of stress corrosion cracking of SPCC steel in brine water.

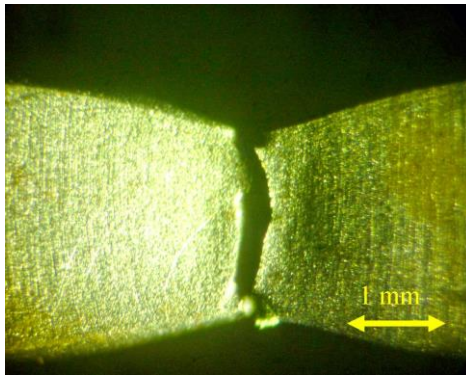
The ultimate strain (as shown in Table. 3) for the specimen in atmospheric environment and 3 wt% brine water were 0.270 and 0.248, respectively. This result ensures that the discrepancy between curves was caused by the concentration of brine water. The sensitivity index of SCC can be evaluated by the mechanical property through the specimens tested in corrosive medium and ambient air as given by the relationship [16, 17]:

$$I_s = \left(1 - \frac{\delta_s}{\delta_0}\right) \times 100\%$$

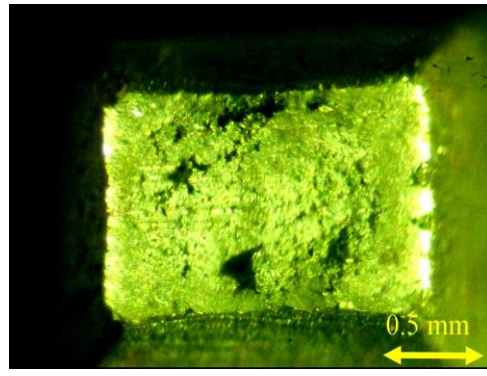
where δ_s and δ_0 are the strain values of the specimen in the brine water and ambient air,

respectively. Apparently, the sensitivity index of the stress corrosion cracking significantly increased with increasing NaCl concentration as shown in Fig. 7. This effect is predominantly attributable to the inferior corrosion resistance of the SPCC steel in the 3 wt% brine water as described in section 3.1.

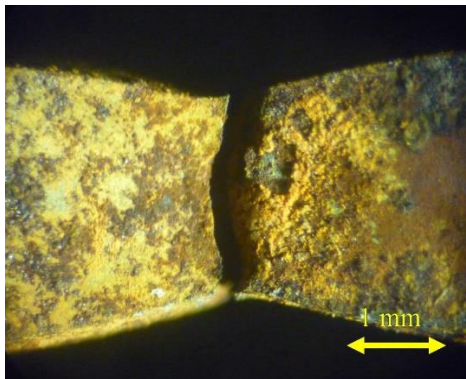
3.3 Fracture surface of the SSRT specimen



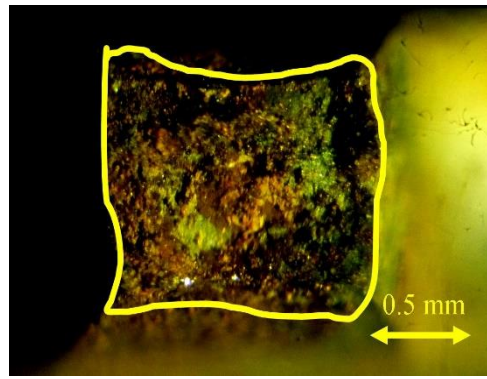
(a) ambient environment



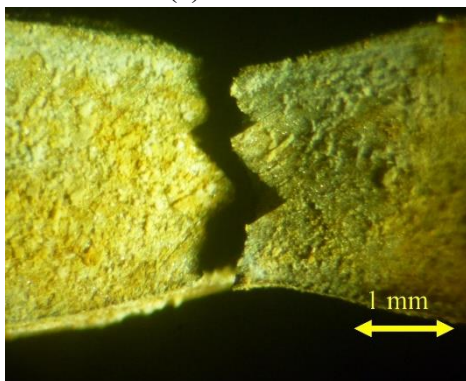
(b) ambient environment



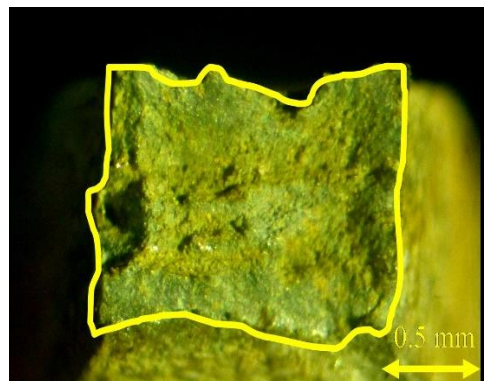
(c) 3 wt%



(d) 3 wt%



(e) 9 wt%



(f) 9 wt%

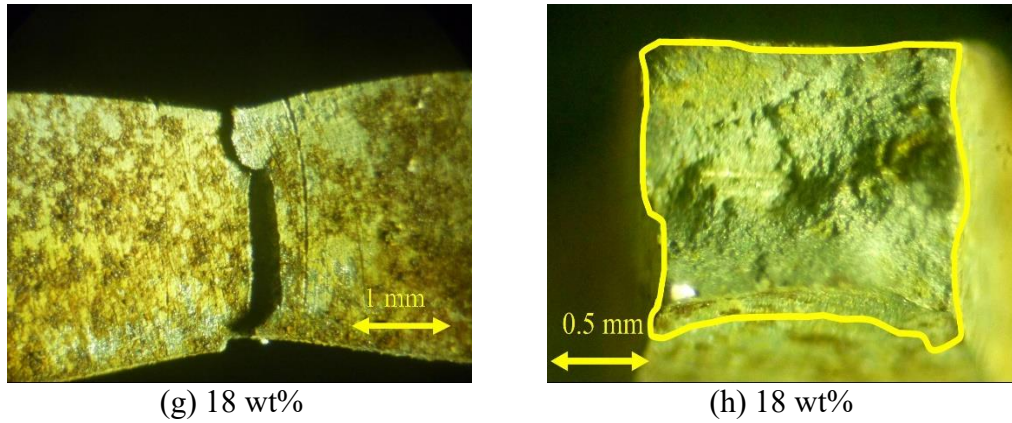


Figure 8. Surface morphology showing details of the specimen subjected to the tensile test at various NaCl solutions. Lateral view (a), (c), (e), (g) and top view (b), (d), (f), (h), (g)

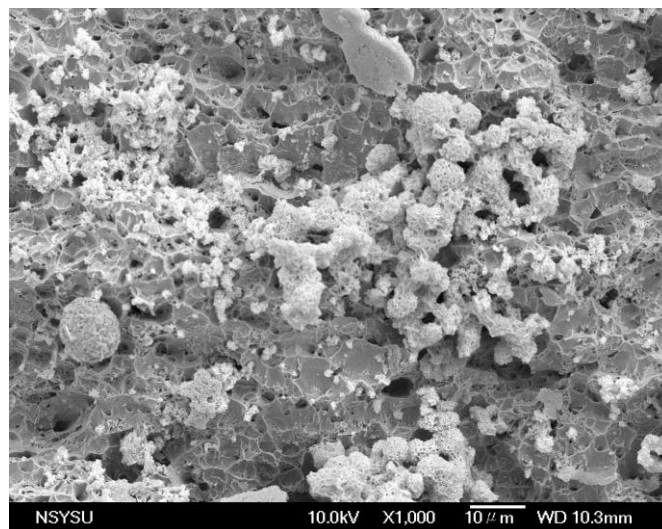
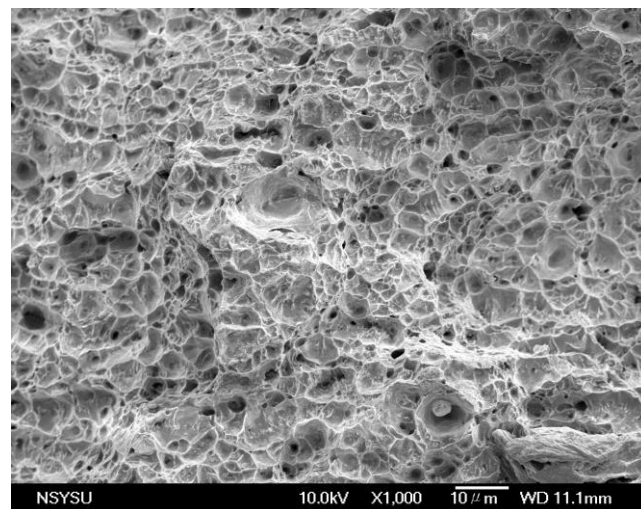


Figure 9. Scanning electron microscope photograph of the fracture surface of SPCC steel after SSRT (strain rate $5.5 \times 10^{-7} \text{ sec}^{-1}$) (a) dimple morphology on the fracture surface in ambient environment (b) partially brittle in 3 wt% brine water

The morphology of the fracture surface was obtained using optical microscopy and scanning electron microscopy (SEM). The smooth (Fig.8(a)) and sawtooth shapes (Fig.8(c), (e) and (g)) of lateral views were caused by the partial and completely ductile behaviour. The presence of an irregular contour (as depicted in Fig. 8(d), (f) and (h)) was observed owing to the corrosion environment and the abundant oxide cover with the fracture surface.

The micrography of the fractured specimen was obtained using SEM as shown in Fig. 9. These specimens showed a minor brittle type and complete ductile fracture due to quasi-cleavage features [16, 18, 20] and the voids caused by cracking, respectively. Because the specimen was in ambient environment, the failure mechanism was associated with ductile deformations owing to the presence of abundant dimples [19] in the fracture zone (Fig. 9(a)). This research demonstrated the difference between the fracture surfaces in brine water and ambient environment. These results are consistent with the reported results by other researchers [18] who have reported that the susceptibility of steel to stress corrosion cracking is strongly dependent on the NaCl concentration, more susceptible to SCC in the 3.5 wt% brine water.

4. CONCLUSION

SCC is a fracture mechanism caused by a synergism between tensile stress and a corrosive environment. The stress corrosion cracking susceptibility was measured by SSRT (*strain rate* $5.5 \times 10^{-7} \text{ s}^{-1}$) in NaCl solution. As the potentiodynamic polarization measurement, the corrosion currents of the specimen subjected to 3 and 18 wt% NaCl were $3.75\text{E}-5$ and $7.44\text{E}-8$ (A/cm^2), respectively. The mechanical property (stress–strain curve) also deteriorated in the brine water, especially in the lower-concentration region. It was proved that the SPCC steel remained in brittle failure and severely corrosive behaviour when exposed to the brine water (NaCl content of 3 wt%). According to microscopic observation, the presence of cleavages and abundant dimples in the fracture zone corresponded to the specimen with and without susceptibility to the brine water, respectively. The present result yields the important conclusion that SPCC steel is sensitive to brine water environment, especially in NaCl content of 3 wt%. This paper is concerned with identifying SPCC steel performance for vehicle structure design, and it provides a preliminary evaluation for a specimen in brine water environment.

ACKNOWLEDGEMENTS

The authors acknowledge support of the Ministry of science and technology, contract no. MOST106-2633-M-017-001.

References

1. Y. Qi, H. Luo, S. Zheng, C. Chen, Z. Lv and M. Xiong, *Int. J. Electrochem. Sci.*, 9 (2014) 2101.
2. Y. Wang, G. Cheng, W. Wu, Q. Qiao, Y. Li and X. Li, *Appl. Surf. Sci.*, 349 (2015) 746.
3. B.H. He, J.J. Sun and Q.A. Tu, *Int. J. Electrochem. Sci.*, 10 (2015) 10631.
4. Y.F. Zhou, W.J. Qiu, W.X. Li and J. Xie, *Adv. Mat. Res.*, 634 (2013) 1698.
5. C.H. Lin, J.R. Lee, H.H. Sheu and S.Y. Tsai, *Int. J. Electrochem. Sci.*, 12 (2017) 7965.

6. W.T. Tsai and M.S. Chen, *Corros. Sci.*, 42 (2000) 545.
7. C.K. Lee, *Int. J. Electrochem. Sci.*, 7 (2012) 8487.
8. H. Liu, *Int. J. Electrochem. Sci.*, 10 (2015) 2130.
9. Y. Li, Z. Liu, L. Ke, L. Huang, C. Du and X. Li, *Int. J. Electrochem. Sci.*, 11 (2016) 5021.
10. B. Li, J. Wang, X. Wang and X. Yue, *Int. J. Electrochem. Sci.*, 11 (2016) 1.
11. Z. Zhu, *Int. J. Electrochem. Sci.*, 11 (2016) 10895.
12. Y. Guo, J. Hu, Y. Jiang and J. Li, *Int. J. Electrochem. Sci.*, 11 (2016) 4812.
13. A. Hassani, A. Habibolahzadeh, A.H. Javadi and S.M. Hosseini, *J. Mater. Eng. Perform.*, 22 (2013) 1783.
14. G.K. Pedraza-Basulto, A.M. Arizmendi-Morquecho, J.A. Cabral Miramontes, A. Borunda-Terrazas, A. Martinez-Villafane and J.G. Chacón-Nava, *Int. J. Electrochem. Sci.*, 8 (2013) 5421.
15. X. Wang, X. Tang, L. Wang, C. Wang and Z. Guo, *Int. J. Electrochem. Sci.*, 9 (2014) 4574.
16. C.J. Ortiz-Alonso, J.G. Gonzalez-Rodriguez, J. Uruchurtu-Chavarin and J.G. Chacon-Nava, *Int. J. Electrochem. Sci.*, 10 (2015) 5249.
17. Q. Guo, J.H. Liu, M. Yu and S.M. Li, *Int. J. Electrochem. Sci.*, 10 (2015) 701.
18. C.S. Brandolt, M.A. Rosa, L.B. Ramos, R.M. Schroeder, C.F. Malfatti and I.L. Müller, *Mater. Sci. Technol.*, 3 (2017) 227.
19. G. Krishnan, A. Varshney, V. Parameswaran and K. Mondal, *J. Mater. Eng. Perform.*, 26 (2017) 2619.
20. M.P. LaCoursiere, D.K. Aidun and D.J. Morrison, *J. Mater. Eng. Perform.*, 26 (2017) 2337.
21. D.A. Jones, *Principles and prevention of corrosion*. Prentice Hall, Inc., (1996) New Jersey, USA.

© 2019 The Authors. Published by ESG (www.electrochemsci.org). This article is an open access article distributed under the terms and conditions of the Creative Commons Attribution license (<http://creativecommons.org/licenses/by/4.0/>).